C_4 photosynthesis and climate through the lens of optimality

Haoran Zhou[a,1], Brent R. Helliker[a], Matthew Huber[b], Ashley Dicks[b], and Erol Akçay[a]

[a]Department of Biology, University of Pennsylvania, Philadelphia, PA 19104; and [b]Department of Earth, Atmospheric, and Planetary Sciences, Purdue University, West Lafayette, IN 47907

Edited by James R. Ehleringer, University of Utah, Salt Lake City, UT, and approved October 10, 2018 (received for review October 31, 2017)

CO_2, temperature, water availability, and light intensity were all potential selective pressures that determined the competitive advantage and expansion of the C_4 photosynthetic carbon-concentrating mechanism over the last ∼30 My. To tease apart how selective pressures varied along the ecological trajectory of C_4 expansion and dominance, we coupled hydraulics to photosynthesis models while optimizing photosynthesis over stomatal resistance and leaf/fine-root allocation. We further examined the importance of nitrogen reallocation from the dark to the light reactions. We show here that the primary selective pressures favoring C_4 dominance changed through the course of C_4 evolution. The higher stomatal resistance and leaf-to-root ratios enabled by C_4 led to an advantage without any initial difference in hydraulic properties. We further predict a reorganization of the hydraulic system leading to higher turgor-loss points and possibly lower hydraulic conductance. Selection on nitrogen reallocation varied with CO_2 concentration. Through paleoclimate model simulations, we find that water limitation was the primary driver for a C_4 advantage, with atmospheric CO_2 as high as 600 ppm, thus confirming molecular-based estimates for C_4 evolution in the Oligocene. Under these high-CO_2 conditions, nitrogen reallocation was necessary. Low CO_2 and high light, but not nitrogen reallocation, were the primary drivers for the mid- to late-Miocene global expansion of C_4. We also predicted the timing and spatial distribution for origins of C_4 ecological dominance. The predicted origins are broadly consistent with prior estimates, but expand upon them to include a center of origin in northwest Africa and a Miocene-long origin in Australia.

C_4 evolution | optimal stomatal conductance | resource allocation | water limitation | dark/light reaction

The evolution of the C_4 photosynthetic pathway enabled the concentration of CO_2 around Rubisco, the enzyme responsible for the first major step of carbon fixation in the C_3 photosynthetic pathway, thus reducing photorespiration. C_3 photosynthesis is present in all plants, but within C_4 plants, the C_3 pathway is typically ensconced within specialized bundle sheath cells that surround leaf veins. CO_2 that diffuses into a leaf is shuttled from adjacent mesophyll cells to the bundle sheath via a four-carbon pump, the energetic cost of which is remunerated by ATP derived from the light reactions (1, 2). As a whole, the C_4 pathway reduces photorespiration, a process that can dramatically reduce photosynthesis and begins with the assimilation of O_2, instead of CO_2, by Rubisco. Over the last 30 My, the reduction in C_3 photosynthesis by photorespiration was large and broad enough to select for the independent evolution of the C_4 pathway more than 60 times across the terrestrial plants (3). The diversity of plant families with C_4 is greatest in the eudicots (1,200 species) and the Poaceae, the monocot family containing the grasses (4,500 species) (2), which accounts for nearly 25% of terrestrial plant productivity and several important agricultural species (4).

While increased photorespiration was central to the evolution of the C_4 carbon concentrating mechanism (CCM), the relative ecological importance of different environmental drivers of the photorespiratory increase is not as clear (5, 6). Lower CO_2 and higher temperature lead to higher rates of photorespiration, which selected for the evolution of C_3–C_4 intermediates and ultimately C_4. Past physiological models, therefore, focused on temperature and CO_2 concentration as selective pressures for C_4 evolution and expansion (7, 8). Under warmer temperatures and low CO_2, C_4 photosynthesis has greater carbon gain than C_3, but under cooler temperatures and high CO_2, the metabolic costs of the C_4 pathway and lower photorespiration in C_3 leads to greater carbon gain in C_3. Alternatively, water availability has been proposed as the impetus for C_4 evolution in eudicots (2), and recent phylogenetic analyses have suggested the same in grasses (6). Water availability should have an impact on C_4 evolution that could work independently or in concert with changes in CO_2 and temperature. First, water deficits indirectly increase photorespiration in C_3 plants by forcing stomatal closure to reduce leaf water loss, consequently decreasing the flux of CO_2 into the leaf and the availability of CO_2 for Rubisco (9). Second, the C_4 CCM allows for the maintenance of lower stomatal conductance, and therefore lower water loss, for a given assimilation rate, leading to a higher water-use efficiency (WUE) than C_3 (10).

The different environmental drivers of the photorespiratory increase in C_4 progenitors—atmospheric CO_2 concentration, temperature, and water availability—changed dramatically over the period of C_4 diversification and expansion. Although there is uncertainty of CO_2 concentration from different proxies (11), atmospheric CO_2 generally decreased from the mid-Oligocene (∼600 ppm) to the ∼400 ppm in the midearly Miocene (12, 13) but with significant variability (±100 ppm; refs. 13 and 14), after which it reduced to values of less than ∼300 ppm in the Pliocene (13). Physiological models that focused on temperature and CO_2 implied that C_4 evolved, in both grasses and eudicots, at the low

Significance

We use a coupled photosynthesis–hydraulic optimal physiology model in conjunction with paleoclimate modeling to examine the primary selective pressures along the ecological trajectory of C_4 photosynthesis and to confirm and revise likely geographical points of dominance and expansion. Water limitation was the primary driver for the initial ecological advantage of C_4 over C_3 in the mid-Oligocene until CO_2 became low enough to, along with light intensity, drive the global expansion of C_4 in the Miocene. Our integrated modeling framework also predicts C_4 evolution should be followed by a decrease in hydraulic conductance, an increase in the leaf–turgor-loss point, and CO_2-dependent reallocation of nitrogen between dark and light reactions.

Author contributions: H.Z., B.R.H., and E.A. designed research; H.Z., B.R.H., M.H., A.D., and E.A. performed research; H.Z., M.H., and E.A. contributed new reagents/analytic tools; H.Z., B.R.H., M.H., A.D., and E.A. analyzed data; and H.Z., B.R.H., M.H., and E.A. wrote the paper.

The authors declare no conflict of interest.

This article is a PNAS Direct Submission.

Data deposition: The source code is available from the Purdue University Research Repository, https://purr.purdue.edu (doi.org/10.4231/R7PR7T75).

[1]To whom correspondence should be addressed. Email: haoranzh@sas.upenn.edu.

This article contains supporting information online at www.pnas.org/lookup/suppl/doi:10.1073/pnas.1718988115/-/DCSupplemental.

Published online November 6, 2018.

end of this CO_2 range in the mid-Miocene to the Pliocene (2, 7, 8, 15). Isotopic and fossil evidence shows that C_4 grasses became a major component of grassland biomes—in terms of biomass, C_4 lineage diversity, or herbivore dietary components—in the mid-Miocene, but molecular evidence suggests that C_4 photosynthesis may have arisen in the grasses as early as the mid-Oligocene, more than 30 Mya (11). Similarly, phylogenetic reconstructions provide evidence that some eudicots evolved C_4 as early as the monocots and also saw the greatest rate of C_4 diversification and expansion in the late Miocene (16, 17). The error associated with these molecular dating techniques is large, however, and the uncertainty range for even the oldest C_4 lineages overlaps with the mid-Miocene estimates for C_4 evolution and expansion. Along with CO_2, precipitation declined over the period of C_4 diversification and expansion, leading to vast terrestrial areas where low or highly seasonal precipitation inputs led to the loss of forests and, consequently, the evolution of the world's first grasslands (18). The spread of grasslands indicates a habitat change with larger surface radiation loads, higher surface temperatures, and increased potential for plant water loss (5, 19). Therefore, if the early evolution of C_4 suggested by molecular-dating approaches are correct, then water availability played an important role for both C_4 grasses and eudicots, while CO_2 was still relatively high (5, 16, 19, 20). The potentially interacting roles of water availability, changes in radiation, and CO_2 along the ecological trajectory of C_4 photosynthesis have not been fully investigated within comprehensive physiological and paleoclimate models.

A related but largely unstudied physiological change during the divergence of C_4 photosynthesis from C_3 is the allocation of nitrogen between the dark reactions and the light reactions. C_4 plants might allocate a greater proportion of N to light reactions than to dark reactions compared with C_3 because of the extra ATP cost of the CCM (21, 22). We propose that the reallocation of N between dark and light reactions provides a further advantage for C_4 above the CCM alone and that different environmental conditions can select for a shift in the degree of reallocation both through evolutionary time and across species in extant plants.

Our goal is to integrate several ecologically relevant selective pressures that determined the competitive advantage and expansion of the C_4 pathway from the mid-Oligocene through to the late Miocene. C_4 evolved via C_3–C_4 intermediates that display a number of successive biochemical and anatomical traits that reduce photorespiration compared with C_3 plants, but further reductions in photorespiration, enhanced WUE and nitrogen-use efficiency, and increases in ecological niche space did not occur until the evolution of the full C_4 CCM (23, 24). We therefore assume that C_3 plants, and not C_3–C_4 intermediates, were the major ecological competitors of C_4 plants. We examine how changes in selective pressures augmented the relative advantage of these two evolutionarily stable states within the framework of an optimality model in which the plant makes allocation "decisions" to maximize photosynthetic assimilation rate. We advance our understanding of C_4 photosynthesis in five ways. First, we revisit the temperature–CO_2 crossover approach and integrate the effects of water limitation, light, optimal allocation decisions, and the interactions between these in a single model. Second, we formalize the hypothesis that C_4 photosynthesis has a higher WUE than C_3, using an optimality argument to balance carbon gain and water loss. Specifically, we let both stomatal conductance and leaf/fine-root allocation emerge endogenously, rather than assuming a priori that C_4 grasses have lower stomatal conductance. This allows us to elucidate the previously unexplored role of optimal stomatal conductance (but see ref. 15) and resource allocation in mediating ecological success due to water limitation and to predict further divergence of hydraulic properties. Third, we explicitly include the additional ATP cost of the C_4 pathway with a mechanistic model (1, 25), which previous modeling analysis did not explicitly consider (7, 8, 19). Fourth, we consider reallocation of nitrogen from the dark reactions to the light reactions, which can change tradeoffs between photosynthesis and water use by C_4. Finally, we drive the optimality model under three CO_2 scenarios with outputs from a fully coupled general circulation model for Miocene/Oligocene climate to examine regions and timing of C_4 ecological advantage as a proxy for potential evolutionary origins.

Results

We validated our optimality model through comparisons with previous models and empirical data from closely related C_3 and C_4 species measured under similar conditions (26) (*SI Appendix*, Fig. S1). Model outputs were consistent with observed patterns of C_3 versus C_4 for stomatal resistance, biomass allocation, photosynthesis, and leaf water potential. Leaf water potential predictions matched observed values, while predicted values for other measures were slightly higher. We incorporated our stomatal resistance and biomass outputs into a Penman–Monteith model to determine if we could replicate the observed ecosystem-level water balance of C_3–C_4 mixed grasslands (27) (*SI Appendix*, *Supporting Information SI3*). Our model confirmed that increasing the C_4 grass component reduces desiccation under higher temperatures and CO_2 (*SI Appendix*, Fig. S2 and Table S3). We further predicted that local desiccation would occur in pure C_3 grasslands due to warming, even with CO_2 increasing from 400 ppm to 600 ppm (*SI Appendix*, Fig. S3). In contrast, local desiccation would be mitigated in pure C_4 grasslands.

Assimilation-based crossover temperatures, defined as the temperature at which assimilation by the C_4 pathway exceeds that of the C_3 pathway, decrease as water limitation increases and light intensity increases across all CO_2 concentrations (Fig. 1 and *SI Appendix*, Fig. S4). Without water stress (solid black line in Fig. 1), our model predicts a C_3/C_4 crossover temperature of 23 °C under 380 ppm, a result similar to previous data and/or models (7, 8). The model results in Fig. 1 were all under the light intensity of 1,400 $\mu mol \cdot m^{-2} \cdot s^{-1}$ and with a C_4 J_{max}/V_{cmax} ratio of 4.5, which corresponds to a reallocation of nitrogen from dark to light reactions. Model results for a C_4 J_{max}/V_{cmax} ratio of 2.1 (no reallocation) were similar (*SI Appendix*, Fig. S4*A*), with the exception of low CO_2 and low water availability. Crossover temperatures are higher with $J_{max}/V_{cmax} = 4.5$, showing that nitrogen

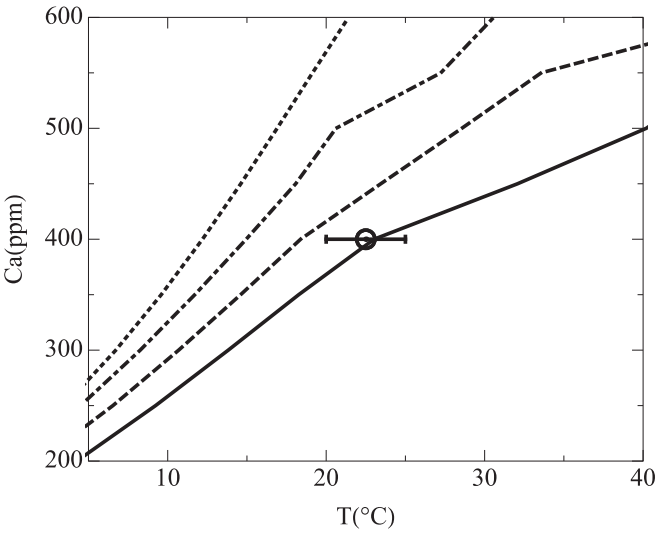

Fig. 1. Crossover temperatures of photosynthesis for C_3 and C_4 with the change of CO_2 concentration under different water conditions. Light intensity was 1,400 $\mu mol \cdot m^{-2} \cdot s^{-1}$ for all model runs. $J_{max}/V_{cmax} = 2.1$ for C_3 and $J_{max}/V_{cmax} = 4.5$ for C_4. Solid black line: VPD = 0.1 kPa, $\psi_s = 0$ MPa; dashed black line: VPD = 0.625 kPa, $\psi_s = -0.5$ MPa; dot-dashed black line: VPD = 1.25 kPa, $\psi_s = -1$ MPa; dotted black line: VPD = 1.875 kPa, $\psi_s = -1.5$ MPa. The circle and error bars indicated the average and confidence intervals of crossover temperature in Collatz (8).

reallocation decreases the C_4 advantage under water limitation and low CO_2. Under saturated soil and low vapour pressure deficit (VPD), crossover temperatures decrease along with increasing light intensity (*SI Appendix*, Fig. S4 *C* and *D*). An increase in light intensity provides a larger relative benefit for C_4 at low CO_2, because C_3 photosynthesis remains CO_2-limited throughout, while C_4 light limitations lessen as light increases. Photosynthetic limitation states were examined under multiple environmental scenarios, using $J_{max}/V_{cmax} = 2.1$ or 4.5 for C_4. With $J_{max}/V_{cmax} = 2.1$, C_4 is light-limited in most conditions (*SI Appendix*, Fig. S5 *A* and *C*). With $J_{max}/V_{cmax} = 4.5$, or when CO_2 decreases to 200 ppm, C_4 becomes limited by CO_2 under low temperatures and by light under high temperatures (*SI Appendix*, Fig. S5 *B* and *D–F*).

To provide a more quantitative measure of C_4 advantage, we calculated the net assimilation rate difference between C_4 and C_3, ΔA_n (net assimilation of C_4 minus that of C_3), through all environmental variations (Fig. 2 and *SI Appendix*, Fig. S6). The positive contour space ($\Delta A_n > 0$) means that C_4 outcompetes C_3 within given environmental dimensions, and the higher the ΔA_n, the greater the advantage of C_4. In Fig. 2, the light intensity of 1,400 $\mu mol \cdot m^{-2} \cdot s^{-1}$ is fixed for all model runs. Under $CO_2 = 200$ ppm, ΔA_n is higher under moist conditions than water-limited conditions (Fig. 2 *A* and *B*). In contrast, under higher CO_2 (400 and 600 ppm), C_4 has the greatest advantage only in water-limited conditions, leaving a relatively small environmental envelope for C_4 (Fig. 2 *C–F*). This is because C_3 photosynthesis has a greater proportional increase in assimilation from 200 to 400 or 600 ppm CO_2. Across all scenarios, increasing J_{max}/V_{cmax} increases both the ΔA_n and space for C_4 advantage (Fig. 2 *B*, *D*, and *F*). Light responses were examined under saturated soils (*SI Appendix*, Fig. S6) and at low CO_2. ΔA_n increases strongly as light increases, whereas there is a much smaller light effect at 400 ppm CO_2 and higher, and a high J_{max}/V_{cmax} was required for a C_4 advantage ($\Delta A_n > 0$).

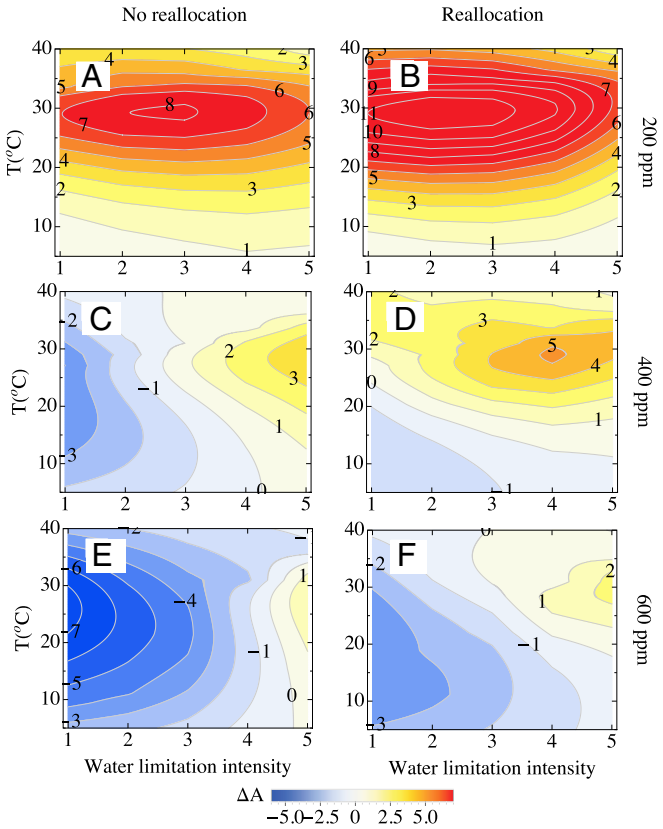

Fig. 2. The total difference in CO_2 assimilation between C_4 and C_3 [$A_n(C_4)$–$A_n(C_3)$] under various CO_2 (200 ppm, 400 ppm, and 600 ppm) and water conditions under light intensity (1,400 $\mu mol \cdot m^{-2} \cdot s^{-1}$). $J_{max}/V_{cmax} = 2.1$ for C_3 and C_4 (*A*, *C*, and *E*) and $J_{max}/V_{cmax} = 2.1$ for C_3 and $J_{max}/V_{cmax} = 4.5$ for C_4 (*B*, *D*, and *F*). Water limitation intensity is as follows: 1, VPD = 0.1 kPa, ψ_s = 0 MPa; 2, 0.625 kPa, −0.5 MPa; 3: 1.25 kPa, and −1 MPa; 4, 1.875 kPa, −1.5 MPa; 5: 2.5 kPa, and −2 MPa.

By driving the optimality model with outputs from the paleoclimate model, we can predict the geographic centers for C_4 ecological dominance as a proxy for C_4 origins. Areas of central Asia, southwest Asia, and northern Africa/Arabia would strongly select for C_4 at 600 ppm CO_2 because of the warm temperatures and arid conditions simulated there (Fig. 3*A*). Southwestern Australia also has a significant land area that would support C_4, and to a lesser extent, so does southwestern North America. As CO_2 decreased to 400 and 270 ppm, the areas mentioned above expanded to strongly support a C_4 ecological advantage with the addition of southern Africa and southern South America (Fig. 3 *B* and *C*). As CO_2 decreased, C_4 favorability maintained a foothold in the semiarid sites and moved into wetter regions, while still requiring warm temperatures for an advantage. At both 400 and 600 ppm, a higher J_{max}/V_{cmax} ratio was required for C_4 to maintain a higher advantage over C_3 (Fig. 3 *A* and *B* and *SI Appendix*, Fig. S7 *A* and *B*). At 270 ppm, C_4 had a broad advantage over C_3 with a lower J_{max}/V_{cmax} ratio (Fig. 3*C* and *SI Appendix*, Fig. S7*C*).

We calculated the photosynthesis rates of the two pathways by only varying the J_{max}/V_{cmax} for C_4 to further examine the pure effect of nitrogen reallocation (Fig. 4). With $J_{max}/V_{cmax} = 2.1$ for both C_3 (solid black line) and C_4 (dashed line), the C_4 assimilation rate is rarely higher than C_3, which indicates C_4 does not have an obvious advantage under current CO_2. However, with $J_{max}/V_{cmax} = 4.5$ for C_4 (dotted line), C_4 has an advantage over C_3 at higher temperatures.

Under all environmental and nitrogen allocation scenarios, optimal stomatal resistance (r_s) and leaf biomass/total biomass of leaf and fine-root allocation (f) are higher in C_4 plants than C_3 plants, and response patterns were similar across CO_2 concentrations (*SI Appendix*, Fig. S8). In addition, f decreases and r_s increases as the intensity of water limitation increases. Results are consistent for C_4 with a J_{max}/V_{cmax} of 2.1 and J_{max}/V_{cmax} of 4.5. The higher r_s in C_4 plants led to a consistently higher water potential than C_3 plants in all simulated conditions (*SI Appendix*, Fig. S1*B*). We also predicted that C_4 plants should have a higher leaf–turgor-loss point than closely related C_3 plants, and we found empirical support for this prediction across four closely related C_3–C_4 clusters (Fig. 5).

Discussion

Based on the conditions under which C_4 plants have the ecological advantage over C_3, our results offer physiological and climatological support for a potential Oligocene ecological dominance of C_4. This finding is in concert with the early ranges of C_4 evolution from molecular-based approaches (16, 17), and we use this ecological dominance as a proxy to identify the regions where C_4 would likely emerge. Isotopic and fossil evidence suggest that C_4 photosynthesis first arose in the mid-Miocene, whereas molecular and phylogenetic approaches suggest that C_4 first arose anywhere from the mid-Miocene to mid-Oligocene (11). Our paleoclimate model broadly represents the environmental conditions for Oligocene to mid-Miocene (12, 28, 29), with high CO_2 conditions representing the mid-Oligocene, and low CO_2 mid-Miocene. We find that environmental conditions favored C_4 plants during the mid-Oligocene (~30 Mya) at warm, arid sites where water limitation acted as the primary selective pressure to increase photorespiration when CO_2 was as high as 600 ppm. The geographic origins predicted by our model and those proposed by others (23) tend to agree, which lends general support to our approach. At the same time, there are important differences that impact both the location and potential age for the evolution of C_4 (Fig. 3). Notably, we find a greatly expanded region of potential origin in northern Africa. Under Oligocene/Miocene climate, northern Africa was arid, but the Tethys sea had not yet closed, and the northwest and the northeast were

PLANT BIOLOGY

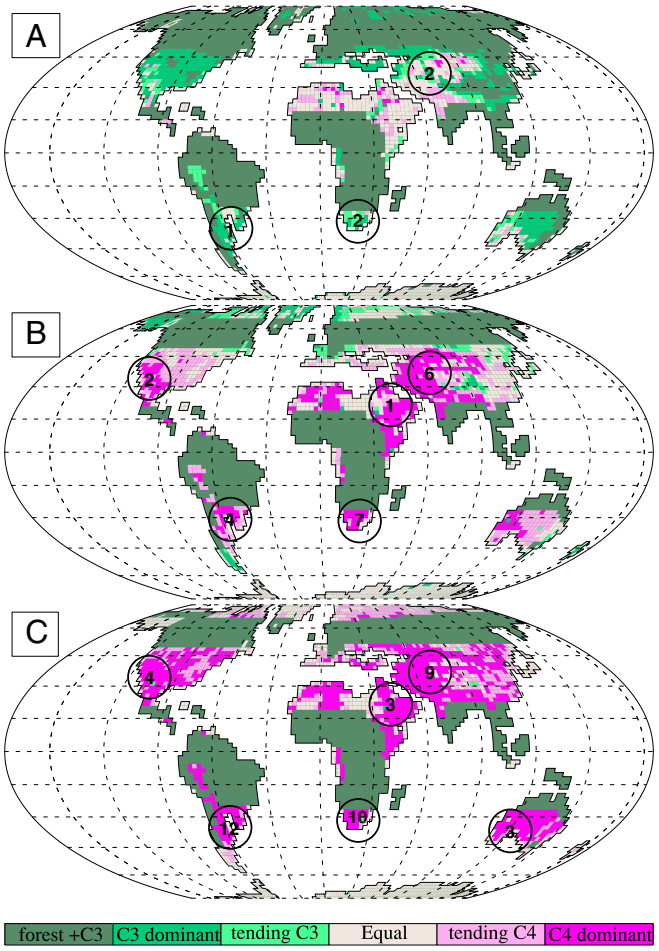

Fig. 3. The regional distributions of C_3 or C_4 ecological dominance under Oligocene/Miocene climate and different CO_2. Dominance is determined by the assimilation difference [$A_n(C_4)$–$A_n(C_3)$; μmol·m^{-2}·s^{-1}] with the thresholds as follows: >3, C_4 dominant; between 1 and 3, C_4 slightly dominant; between −1 and 1, equal dominance; between −3 and −1, C_3 slightly dominant; < −3, C_3 dominant. For each grid cell, the optimality model was driven with outputs from the Community Land Model (CLM4.5) in the CESM: (*A*) 600 ppm CO_2 and (*B*) 400 ppm CO_2, both with C_3 J_{max}/V_{cmax} ratio = 2.1 and C_4 J_{max}/V_{cmax} ratio = 4.5, (*C*) 270 ppm CO_2, C_3 J_{max}/V_{cmax} ratio = 2.1 and C_4 J_{max}/V_{cmax} ratio = 2.1. Circles superimposed on figures indicate evolutionary origins from previous studies (23) and numbers within the circles indicate cumulative lineages within which C_4 evolved by a given time period for (*A*) late Oligocene/early Miocene, (*B*) mid-Miocene, and (*C*) late Miocene/Pliocene.

consequently just wet enough to ecologically favor C_4 over C_3 plants. Likewise, Australia is thought to have developed conditions favorable for the evolution and expansion of C_4 only within the last 9 Mya (23), yet we show it slightly favoring C_4 under Oligocene CO_2 and strongly favoring C_4 by the mid-Miocene. Climate simulations suggest that both northern Africa and southwestern Australia had wetter summers than the current Mediterranean-type climate.

As CO_2 decreased through the Miocene, warm temperatures remained a strong selective force, but the primary selective force for a C_4 advantage over C_3 shifted from water limitation to low CO_2 and, to a lesser extent, light intensity. However, as increased light intensity alone could not lead to an advantage of C_4 under high CO_2 (*SI Appendix*, Fig. S6*C*), it seems likely that C_4 could not dominate except in locally arid areas while CO_2 was high. Thus, after its emergence, C_4 radiation likely idled in small pockets of selective favorability as CO_2 concentrations declined through the Miocene (13), similar to the "edaphic ghetto" hypothesis (30). Furthermore, given that CO_2 may have been rapidly cycling on orbital time scales between 500 ppm and 300 ppm (14), the transition to widespread C_4 could have exhibited hysteresis and occurred through fits and starts. Such shifts in primary selective pressures on C_4 photosynthesis over evolutionary time are consistent with the isotopic evidence (31, 32).

Consistent with previous studies, our model predicts that low CO_2 (200–300 ppm) strongly favors C_4 over C_3 photosynthesis (e.g., refs. 7 and 15). We further show that low CO_2 provides a clear C_4 advantage under a large range of water availability and light intensity regimes. Under low CO_2, the greatest C_4 advantage occurs in relatively moist and mildly water-limited conditions, opposite to that which is seen under high CO_2. Under low CO_2, new C_4 species evolved in multiple lineages and together with the earlier C_4 species started to increase their biomass to occupy open sites (11). The environmental conditions that led to the largest C_4 advantage within our model, therefore, parallel those documented in extant C_4-dominated grasslands: highly seasonal precipitation that occurs chiefly within a warm growing season (33, 34). These are also similar to the conditions that led to the large-scale expansion of C_4 grasslands in the Miocene—for example, the onset of summer monsoons and subsequent C_4 grassland expansion in the Indian subcontinent (35).

The role of water limitation in C_4 grass evolution has sparked interest in grass hydraulics and the anatomical shifts in C_3 grasses that were prerequisites to C_4 evolution (19, 20), and we further propose that the evolution of C_4 photosynthesis leads to a reorganization of the hydraulic system. A lower leaf–turgor-loss point is typically a strong indicator of drought tolerance across species (36). On the contrary, we predict that the higher stomatal resistance of the C_4 CCM leads to a higher leaf water potential than C_3 in all water-limited conditions; thus, there is no need for C_4 to maintain a lower leaf–turgor-loss point. We confirmed this prediction in four closely related C_3–C_4 clusters (Fig. 5). It is thought that the higher vein density of C_4 grasses should lead to greater hydraulic conductance (19, 20), but we found a clear C_4 advantage solely by allowing for optimal leaf:fine-root allocation and stomatal conductance. We also find that increasing hydraulic conductance had little impact on the C_4 advantage (*SI Appendix*, Fig. S9), indicating that the C_4 CCM itself is enough to result in greater carbon gain under water stress. These results do not contradict the idea that larger bundle sheaths and smaller interveinal distance—which were clear prerequisites for C_4 evolution (20, 37)—led to greater hydraulic conductance and drought tolerance among C_4 progenitors (20). They do, however, suggest that greater hydraulic conductance is not necessary to give C_4 plants an advantage once the CCM evolved. We hypothesize that once C_4 evolves in a lineage, selection on increased hydraulic conductance would not only lessen but invert, leading to the development of even narrower xylem conduits and greater drought resistance. There is empirical support for such a prediction in eudicots (38).

Different environmental conditions can select for a shift in the degree of nitrogen allocation across the light and dark reactions

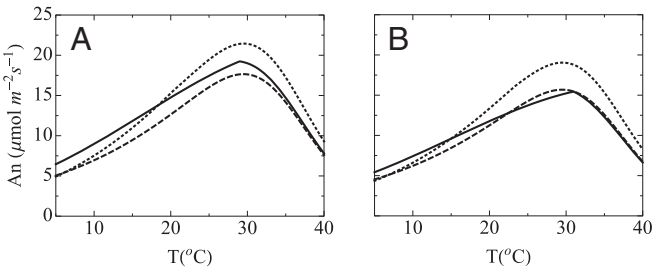

Fig. 4. Assimilation rates of C_3 with J_{max}/V_{cmax} = 2.1 (solid black line), C_4 with J_{max}/V_{cmax} = 2.1 (dashed black line), and C_4 with J_{max}/V_{cmax} = 4.5 (dotted black line) (other parameters are maintained the same for C_3 and C_4) under light intensity of 1,400 μmol·m^{-2}·s^{-1}, CO_2 of 400 ppm, and different water limitation conditions. (*A*) VPD = 0.625 kPa, ψ_s = −0.5 MPa; (*B*) 1.25 kPa, −1 MPa.

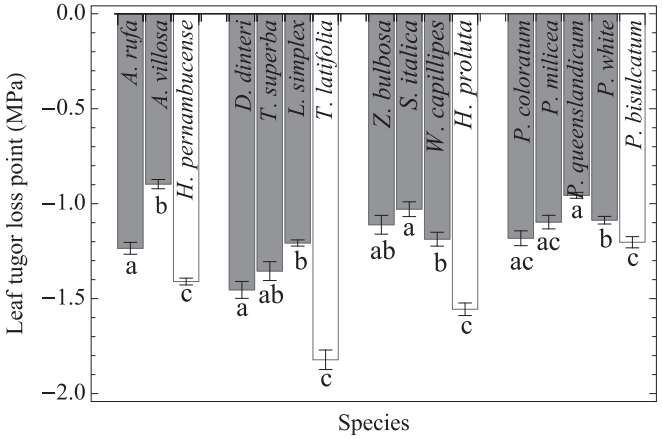

Fig. 5. Measured leaf–turgor-loss points in four closely related groups of C_3 and C_4 species (white bars: C_3 species; gray bars: C_4 species). Error bars show SEs. Different letters denote a significant difference within a group.

separately from the C_4 CCM (assessed here by a change in J_{max}/V_{cmax}). In general, CCMs allow for less investment in nitrogen-rich Rubisco (39), and the nitrogen not used for Rubisco could be either reinvested in light-harvesting machinery or simply not used at all, thus reducing the total nitrogen requirement. Modeling studies have long assumed a high J_{max}/V_{cmax} for C_4 photosynthesis (19, 40), and measurements show lower Rubisco content and higher chlorophyll and thylakoid content, giving evidence of reallocation in extant C_4 species (21, 22). Empirical estimates of J_{max}/V_{cmax}, in C_4 plants, are more variable, ranging from 2 to above 6, with a mean of around 4.5 (41–43), which is higher than the mean J_{max}/V_{cmax} estimates for C_3 plants of 2.1 (44). Increasing J_{max}/V_{cmax} almost always increases the photosynthesis rate of C_4 grasses (Fig. 4 and *SI Appendix*, Fig. S10) and therefore could lead to a competitive advantage over C_3 grasses as well as C_4 grasses that do not reallocate. Assuming there is little cost or no genetic constraints for reallocation, the selection pressure to reallocate would have been strongest when CO_2 was high because the CCM alone does not give C_4 a large advantage. When CO_2 was low during the late Miocene C_4 expansion, however, the CCM alone would give C_4 an advantage and reallocation would not change the competitive balance between C_3 and C_4. As CO_2 remained low through to the Pleistocene, selection for nitrogen reallocation to the light reactions would lessen further, especially during the CO_2 minima of the Pleistocene glacial periods (~180 ppm).

Each evolutionary origin of C_4 photosynthesis represents both different selective pressures and taxonomic (genetic) constraints as climate and CO_2 changed. Taking the Chloridoideae as an example, we can use our model to develop hypotheses along the ecological trajectory of C_4 in this grass subfamily. The ecological advantage of C_4 photosynthesis in the Oligocene, while CO_2 was high, was driven by aridity, acting to decrease stomatal conductance that increased photorespiration in C_4 progenitors initially, and led to higher WUE upon the evolution of the CCM. There would have been enough of a reduction in water use that the turgor-loss point would increase and selection for increased hydraulic conductance would relax, allowing for the development of more resilient—and less conductive—xylem. There would have been strong selection for reallocation of nitrogen from the dark reactions to the light reactions. The large radiation of C_4 within the Chloridoideae occurring in the mid- to late Oligocene was likely driven by low CO_2 and high light, and the previously evolved hydraulic resilience would perhaps relegate this subfamily to being the dry-site specialists observed in current-day distributions (45). There would have been much less selective pressure to reallocate N during the large radiation, but such a reorganization was likely already in place within the clade. In contrast, for the lineages that evolved C_4 in the late Miocene (e.g., *Stipagrostis*, *Eriachne*, *Neurachne*), CO_2 would have been the primary impetus for C_4 evolution, but for these lineages, there would have been little selection to reallocate nitrogen, and we predict that they would have greater hydraulic conductance and lower turgor-loss points than those of the Chloridoideae.

By optimizing carbon gain over water loss, we developed a plausible physiological explanation for the ecological advantage of C_4 through time and further proposed hypotheses about how a variety of traits that accompany the C_4 CCM developed in concert with the climate changes that occurred through this ecological trajectory (46). There are obvious caveats with our interpretations, because we focus solely on physiology and assume that competitive outcomes or selective pressures are decided primarily by photosynthetic rates. We also do not consider how larger ecological processes like disturbance can undermine physiology-based projections of plant distributions (47). However, by examining extant species within select lineages in both controlled and natural environments, these hypotheses can be examined empirically together with our physiological model, ultimately providing an integrative view of the selection pressures that led to the current physiologies and distribution of C_4 plants.

Materials and Methods

Overview of the Plant Model. We first assume that the CCM is the only difference between C_3 and C_4, corresponding to two closely related species whose other traits have not yet diverged. We then allow for divergence through shifts in nitrogen allocation between the light and dark reactions of C_4. Our model incorporates the soil–plant–air–water continuum into traditional C_3 (48) and C_4 (25) photosynthesis models and assumes that plants optimize stomatal resistance and leaf/fine-root allocation to balance carbon gain and water loss (49). The rate of water loss through transpiration equals the rate of water absorption by the roots, at equilibrium (49). Stomatal resistance (r_s) controls transpiration and photosynthesis. The leaf/fine-root (f) ratio, defined as the ratio of biomass for leaves to the sum of biomasses for leaves and fine roots, controls the biomass allocated to leaf area for transpiration and photosynthesis. The lowering of leaf water potential through transpiration water loss and/or environmental factors (VPD and soil water potential) leads to a lowering of the photosynthetic rate via Weibull-type vulnerability curves (40). A full model description is in *SI Appendix, Supporting Information SI1* with *SI Appendix*, Table S1 for parameter abbreviations and *SI Appendix*, Table S2 for input parameters. The model derivation and methods for numerical solutions using Mathematica (Wolfram Research, Inc.)/R are in *SI Appendix*, Mathematica-S1 and R package.

Optimal Stomatal Resistance and Allocation of Energy Between Leaves and Fine Roots. We assume that the plant adjusts the rs and f to optimize the total carbon gain

$$A_{total} = \frac{fNA_n}{\rho},$$

where ρ is the leaf mass density ($g \cdot m^{-2}$), and for simplicity, we assume that N and ρ are fixed (49). This amounts to considering the optimization problem faced by the plant in a given instance during growth, where size is a constant. We treat the instantaneous optimization problem as a proxy for the optimal growth path as the growth rate is maximized at any given time. We regard ρ as a species-specific trait that changes at a slower time scale than rs and f.

Allocation of Nitrogen. The ratio J_{max}/V_{cmax} was used as a proxy for nitrogen allocation between RuBP carboxylation and regeneration. The initial condition for J_{max}/V_{cmax} was 2.1 (44) for both C_3 and C_4. For the reallocation, the value for C_4 is $J_{max}/V_{cmax} = 4.5$ (19, 40). We used a simple stoichiometry for J_{max} and V_{cmax} by considering the sum of J_{max} and V_{cmax} as a constant representing total available nitrogen for photosynthesis; such a stoichiometry was drawn from the existing modeling work (19, 40). Two assumptions underlie this stoichiometry: (*i*) Investing one molecule of N to the dark reactions increases V_{cmax} to the same degree as investing one molecule of N to the light reactions increases J_{max}, and (*ii*) nitrogen allocation to enzymes involved in photorespiration (C_3) and the CCM (C_4) offset each other. These simplified assumptions are meant to represent an initial analysis of the effect of reallocation; they can be further adjusted when more detailed stoichiometry is available.

PLANT BIOLOGY

Modeling Scenarios. Photosynthesis was modeled over the following ranges of environmental conditions: 10 °C to 40 °C with 0.125 °C intervals; CO_2 200 ppm to 600 ppm with 50 ppm intervals; water conditions VPD = 0.1, 0.625, 1.25, 1.875, and 2.5 kPa, with corresponding soil water potential (ψ_s) = 0, −0.5, −1, −1.5, and −2 MPa and light intensities 1,400, 1,000, 600, 200, and 100 $\mu mol \cdot m^{-2} \cdot s^{-1}$. We consider VPD = 0.1 kPa and ψ_s = 0 MPa as saturated and light intensity of 1,400 $\mu mol \cdot m^{-2} \cdot s^{-1}$ as an average light intensity of a day in open habitat. Environmental factors are intended to reflect growing-season averages.

Paleoclimate Modeling of Geographic Centers of Evolution. Building on existing boundary conditions and simulations using earlier versions of the National Center for Atmospheric Research (NCAR) coupled model (The Community Climate System Model, versions 3 and 4), we implement mid-Miocene simulations in Community Earth System Model (CESM) 1.0.5 (50) incorporating slightly updated boundary conditions (51) within CESM incorporating the Community Atmosphere Model, version 5 atmospheric component (52) and the CLM4 land surface model (53) (*SI Appendix, Supporting Information SI2*).

To drive the vegetation model, growth-season means of atmospheric incident solar radiation, 2 m relative humidity, soil water potential (upper six layers), and daily maximum of average 2 m temperature were generated from 30-y climatological monthly means of CLM output. These fields were masked to include grid cells in the growing season (temperature > 10 °C) and for "open" settings—that is, for grid cells made up of >20% of grassland, shrub-land, woodland, and desert based on the distributions in Herold et al. (51), thus filtering out closed-canopy forests and cold regions. Coding was performed in the NCAR Command Language (NCL); the source code is available from the Purdue University Research Repository https://purr.purdue.edu.

ACKNOWLEDGMENTS. We sincerely thank the constructive comments from the anonymous reviewers. We are grateful for support from the University of Pennsylvania. The simulations were funded by the NSF P2C2 program Award OCE-1602905 (to M.H.) and carried out at Purdue University Rosen Center for Advanced Computing. The NCAR CESM model development is supported by NSF.

1. Hatch MD (1987) C_4 photosynthesis: A unique blend of modified biochemistry, anatomy and ultrastructure. *Biochim Biophys Acta* 895:81–106.
2. Sage RF (2004) The evolution of C4 photosynthesis. *New Phytol* 161:341–370.
3. Grass Phylogeny Working Group II (2012) New grass phylogeny resolves deep evolutionary relationships and discovers C_4 origins. *New Phytol* 193:304–312.
4. Still CJ, Berry JA, Collatz GJ, DeFries RS (2003) Global distribution of C_3 and C_4 vegetation: Carbon cycle implications. *Global Biogeochem Cycles* 17:6-1–6-14.
5. Edwards EJ, Smith SA (2010) Phylogenetic analyses reveal the shady history of C_4 grasses. *Proc Natl Acad Sci USA* 107:2532–2537.
6. Edwards EJ, Still CJ (2008) Climate, phylogeny and the ecological distribution of C_4 grasses. *Ecol Lett* 11:266–276.
7. Ehleringer JR, Cerling TE, Helliker BR (1997) C_4 photosynthesis, atmospheric CO_2, and climate. *Oecologia* 112:285–299.
8. Collatz GJ, Berry JA, Clark JS (1998) Effects of climate and atmospheric CO_2 partial pressure on the global distribution of C_4 grasses: Present, past, and future. *Oecologia* 114:441–454.
9. Flexas J, Bota J, Loreto F, Cornic G, Sharkey TD (2004) Diffusive and metabolic limitations to photosynthesis under drought and salinity in $C_{(3)}$ plants. *Plant Biol (Stuttg)* 6:269–279.
10. Ghannoum O (2009) C_4 photosynthesis and water stress. *Ann Bot* 103:635–644.
11. Edwards EJ, et al.; C4 Grasses Consortium (2010) The origins of C_4 grasslands: Integrating evolutionary and ecosystem science. *Science* 328:587–591.
12. Super JR, et al. (2018) North Atlantic temperature and pCO2 coupling in the early-middle Miocene. *Geology*, 46:519–522.
13. Royer DL (2006) CO_2-forced climate thresholds during the Phanerozoic. *Geochim Cosmochim Acta* 70:5665–5675.
14. Greenop R, Foster GL, Wilson PA, Lear CH (2014) Middle Miocene climate instability associated with high-amplitude CO_2 variability. *Paleoceanography* 29:845–853.
15. Way DA, Katul GG, Manzoni S, Vico G (2014) Increasing water use efficiency along the C_3 to C_4 evolutionary pathway: A stomatal optimization perspective. *J Exp Bot* 65:3683–3693.
16. Vicentini A, Barber JC, Aliscioni SS, Giussani LM, Kellogg EA (2008) The age of the grasses and clusters of origins of C_4 photosynthesis. *Glob Change Biol* 14:2963–2977.
17. Christin PA, Osborne CP, Sage RF, Arakaki M, Edwards EJ (2011) $C_{(4)}$ eudicots are not younger than $C_{(4)}$ monocots. *J Exp Bot* 62:3171–3181.
18. Strömberg CAE (2011) Evolution of grasses and grassland system. *Annu Rev Earth Planet Sci* 39:517–544.
19. Osborne CP, Sack L (2012) Evolution of C_4 plants: A new hypothesis for an interaction of CO_2 and water relations mediated by plant hydraulics. *Philos Trans R Soc Lond B Biol Sci* 367:583–600.
20. Griffiths H, Weller G, Toy LF, Dennis RJ (2013) You're so vein: Bundle sheath physiology, phylogeny and evolution in C_3 and C_4 plants. *Plant Cell Environ* 36:249–261.
21. Tissue DT, Griffin KL, Thomas RB, Strain BR (1995) Effects of low and elevated CO_2 on C_3 and C_4 annuals: II. Photosynthesis and leaf biochemistry. *Oecologia* 101:21–28.
22. Ghannoum O, Evans JR, von Caemmerer S (2010) Nitrogen and water use efficiency of C4 plants. *C4 Photosynthesis and Related CO2 Concentrating Mechanisms*, eds Raghavendra AS, Sage RF (Springer Science, Dordrecht, The Netherlands), pp 129–146.
23. Sage RF, Monson RK, Ehleringer JR, Adachi S, Pearcy RW (2018) Some like it hot: The physiological ecology of C_4 plant evolution. *Oecologia* 187:941–966.
24. Lundgren MR, et al. (2015) Photosynthetic innovation broadens the niche within a single species. *Ecol Lett* 18:1021–1029.
25. von Caemmerer S (2000) Biochemical models of photosynthesis. *Techniques in Plant Sciences* (CSIRO Publishing, Colingwood, Australia), pp 91–122.
26. Taylor SH, et al. (2010) Ecophysiological traits in C_3 and C_4 grasses: A phylogenetically controlled screening experiment. *New Phytol* 185:780–791.
27. Morgan JA, et al. (2011) C_4 grasses prosper as carbon dioxide eliminates desiccation in warmed semi-arid grassland. *Nature* 476:202–205.
28. Lunt DJ, Ross I, Hopley PJ, Valdes PJ (2007) Modelling late Oligocene C_4 grasses and climate. *Palaeogeogr Palaeoclimatol Palaeoecol* 251:239–253.
29. Goldner A, Herold N, Huber M (2014) The challenge of simulating the warmth of the mid-Miocene climatic optimum in CESM1. *Clim Past* 10:523–536.
30. Bond WJ (2015) Fires in the Cenozoic: A late flowering of flammable ecosystems. *Front Plant Sci* 5:749.
31. Cotton JM, Cerling TE, Hoppe KA, Mosier TM, Still CJ (2016) Climate, CO_2, and the history of North American grasses since the Last Glacial Maximum. *Sci Adv* 2:e1501346.
32. Griffith DM, Cotton JM, Powell RL, Sheldon ND, Still CJ (2017) Multi-century stasis in C_3 and C_4 grass distributions across the contiguous United States since the industrial revolution. *J Biogeogr* 44:2564–2574.
33. Hattersley PW (1983) The distribution of C_3 and C_4 grasses in Australia in relation to climate. *Oecologia* 57:113–128.
34. Paruelo JM, Lauenroth WK (1996) Relative abundance of plant functional types in grasslands and shrublands of North America. *Ecol Appl* 6:1212–1224.
35. Quade J, Cerling TE, Bowman JR (1989) Development of Asian monsoon revealed by marked ecological shift during the latest Miocene in northern Pakistan. *Nature* 342:163–166.
36. Bartlett MK, Scoffoni C, Sack L (2012) The determinants of leaf turgor loss point and prediction of drought tolerance of species and biomes: A global meta-analysis. *Ecol Lett* 15:393–405.
37. Christin PA, et al. (2013) Anatomical enablers and the evolution of C_4 photosynthesis in grasses. *Proc Natl Acad Sci USA* 110:1381–1386.
38. Kocacinar F, Sage RF (2003) Photosynthetic pathway alters xylem structure and hydraulic function in herbaceous plants. *Plant Cell Environ* 26:2015–2026.
39. Ku MSB, Schmitt MR, Edwards GE (1979) Quantitative determination of RuBP carboxylase-orygenase protein in leaves of several C_3 and C_4 plants. *J Exp Bot* 114:89–98.
40. Vico G, Porporato A (2008) Modelling C_3 and C_4 photosynthesis under water-stressed conditions. *Plant Soil* 313:187–203.
41. Massad RS, Tuzet A, Bethenod O (2007) The effect of temperature on $C_{(4)}$-type leaf photosynthesis parameters. *Plant Cell Environ* 30:1191–1204.
42. Ye ZP, Suggett DJ, Robakowski P, Kang HJ (2013) A mechanistic model for the photosynthesis-light response based on the photosynthetic electron transport of photosystem II in C_3 and C_4 species. *New Phytol* 199:110–120.
43. Ge ZM, Zhang LQ, Yuan L, Zhang C (2014) Effects of salinity on temperature-dependent photosynthetic parameters of a native C_3 and a non-native C_4 marsh grass in the Yangtze Estuary, China. *Photosynthetica* 52:484–492.
44. Wullschleger SD (1993) Biochemical limitations to carbon assimilation in C_3 plants–A retrospective analysis of the A/C_i curves from 109 species. *J Exp Bot* 44:907–920.
45. Liu H, Edwards EJ, Freckleton RP, Osborne CP (2012) Phylogenetic niche conservatism in C_4 grasses. *Oecologia* 170:835–845.
46. Christin PA, Osborne CP (2014) Tansley review. The evolutionary ecology of C_4 plants. *New Phytol* 204:765–781.
47. Griffith DM, et al. (2015) Biogeographically distinct controls on C_3 and C_4 grass distributions: Merging community and physiological ecology. *Glob Ecol Biogeogr* 24:304–313.
48. Farquhar GD, Von Caemmerer S, Berry JA (1980) A biochemical model of photosynthetic CO_2 assimilation in leaves of C_3 pathway species. *Planta* 149:78–90.
49. Givnish TJ (1986) Optimal stomatal conductance, allocation of energy between leaves and roots, and the marginal cost of transpiration. *On the Economy of Plant Form and Function*, ed Givnish TJ (Cambridge Univ Press, Cambridge, UK), pp 171–213.
50. Hurrell JW, et al. (2013) The community earth system model: A framework for collaborative research. *Bull Am Meteorol Soc* 94:1339–1360.
51. Herold N, Huber M, Mueller RD (2011) Modeling the Miocene climatic optimum. Part I: Land and atmosphere. *J Clim* 24:6353–6372.
52. Neale RB, et al. (2012) Description of the NCAR Community Atmosphere Model (CAM 5.0). *NCAR Technical Note NCAR/TN-486+STR* (National Center for Atmospheric Research, Boulder, CO).
53. Lawrence DM, et al. (2012) The CCSM4 land simulation, 1850–2005: Assessment of surface climate and new capabilities. *J Clim* 25:2240–2260.